Heparin-binding EGF-like growth factor and ErbB signaling is essential for heart function

Ryo Iwamoto*†, Satoru Yamazaki*†, Masanori Asakura†‡, Seiji Takashima†‡, Hidetoshi Hasuwa*, Kenji Miyado*, Satoshi Adachi*, Masafumi Kitakaze§, Koji Hashimoto¶, Gerhard Raab‖, Daisuke Nanba, Shigeki Higashiyama**, Masatsugu Hori‡, Michael Klagsbrun‖, and Eisuke Mekada*††**

*Department of Cell Biology, Research Institute for Microbial Diseases, Osaka University, Suita, Osaka 565-0871, Japan; ‡Department of Internal Medicine and Therapeutics, Osaka University Graduate School of Medicine, Suita, Osaka 565-0871, Japan; §Cardiovascular Division of Medicine, National Cardiovascular Center of Japan, Suita, Osaka 565-0873, Japan; ‖Departments of Surgery and Pathology, Children's Hospital and Harvard Medical School, Boston, MA 02115; and Departments of ¶Dermatology and **Medical Biochemistry, Ehime University School of Medicine, Ehime 791-0295, Japan

Edited by Joan Massagué, Memorial Sloan–Kettering Cancer Center, New York, NY, and approved January 14, 2003 (received for review December 10, 2002)

The heparin-binding epidermal growth factor (EGF)-like growth factor (HB-EGF) is a member of the EGF family of growth factors that binds to and activates the EGF receptor (EGFR) and the related receptor tyrosine kinase, ErbB4. HB-EGF-null mice ($HB^{del/del}$) were generated to examine the role of HB-EGF *in vivo*. More than half of the $HB^{del/del}$ mice died in the first postnatal week. The survivors developed severe heart failure with grossly enlarged ventricular chambers. Echocardiographic examination showed that the ventricular chambers were dilated and that cardiac function was diminished. Moreover, $HB^{del/del}$ mice developed grossly enlarged cardiac valves. The cardiac valve and the ventricular chamber phenotypes resembled those displayed by mice lacking EGFR, a receptor for HB-EGF, and by mice conditionally lacking ErbB2, respectively. HB-EGF–ErbB interactions in the heart were examined *in vivo* by administering HB-EGF to WT mice. HB-EGF induced tyrosine phosphorylation of ErbB2 and ErbB4, and to a lesser degree, of EGFR in cardiac myocytes. In addition, constitutive tyrosine phosphorylation of both ErbB2 and ErbB4 was significantly reduced in $HB^{del/del}$ hearts. It was concluded that HB-EGF activation of receptor tyrosine kinases is essential for normal heart function.

The ErbB family of receptor tyrosine kinases have fundamental roles in development, proliferation, and differentiation (1). There are four members of the receptor tyrosine kinase ErbB family, EGFR/ErbB1/HER1, ErbB2/HER2/neu, ErbB3/HER3, and ErbB4/HER4. Epidermal growth factor (EGF) family ligands bind to and activate their receptors by inducing the formation of homodimers and heterodimers, resulting in autophosphorylation of specific tyrosine residues within the cytoplasmic domain. The phosphorylated tyrosine residues bind adapter proteins, which are instrumental in mediating downstream signaling pathways that determine the biological activity of the ErbB family of ligands.

In vertebrates, the EGF family of ligands bind to ErbB receptors with some degree of preference. EGF, transforming growth factor-α, and amphiregulin bind to EGF receptor (EGFR); heparin-binding EGF-like growth factor (HB-EGF), epiregulin, and betacellulin bind to both EGFR and ErbB4; NRG-1 (neuregulin/heregulin/NDF) and NRG-2 bind to ErbB3 and ErbB4; and NRG-3 and NRG-4 bind to ErbB4 but not to ErbB3. Although no ligand for ErbB2 has yet been described, ErbB2 is active as a signaling receptor by forming heterodimers with other ErbB receptors (2).

HB-EGF is synthesized as a type I transmembrane protein (proHB-EGF) composed of signal peptide, heparin-binding, EGF-like, juxtamembrane, transmembrane, and cytoplasmic domains (3, 4). The membrane-bound proHB-EGF is cleaved at the juxtamembrane domain, resulting in the shedding of soluble HB-EGF (5). The full-length proHB-EGF is biologically active as a juxtacrine growth factor that signals neighboring cells in a nondiffusible manner (6–8). ProHB-EGF forms complexes with CD9 (9) and integrin $\alpha3\beta1$ (10) on the cell membrane. ProHB-EGF is also the receptor for diphtheria toxin, and it mediates the entry of diphtheria toxin into the cytoplasm (11, 12). Soluble HB-EGF is a potent mitogen and chemoattractant for a number of cell types, including vascular smooth muscle cells, fibroblasts, and keratinocytes (13, 14). HB-EGF has been implicated in a number of physiological and pathological processes, which include wound healing (15, 16), cardiac hypertrophy (17), smooth muscle cell hyperplasia (18), kidney collecting duct morphogenesis (19), blastocyst implantation (20), pulmonary hypertension (21), and oncogenic transformation (22).

HB-EGF signaling is complex. HB-EGF activates EGFR (3) and ErbB4 (23) directly but can also activate ErbB2 and ErbB3 indirectly by heterodimerization. Recently, N-arginine dibasic convertase associated with the cell surface has been identified as a specific receptor for HB-EGF, which enhances HB-EGF-induced cell migration by means of EGFR (24). An interesting recent discovery is that HB-EGF, alone among the EGFR ligands, plays a critical role in transactivation of EGFR by G protein-coupled receptor ligands such as lysophosphatidic acid, endothelin-1, and angiotensin-II. The ectodomain shedding of HB-EGF is required for this process (25, 26). This HB-EGF-mediated process contributes to cardiomyocyte hypertrophy (17).

Gene-targeted mouse studies indicate that the ErbB receptor tyrosine kinases are critical for normal heart development. EGFR-null mice with a CD1 background and EGFR mutant (*waved-2*) mice exhibit semilunar valve enlargement (27). ErbB2-null mouse embryos die from a defect in trabecula formation (28). ErbB4-knockout mice are also embryonic lethal because of a similar abnormal trabecula formation, as are mice lacking NRG, the ErbB4 ligand (29, 30). Disruption of the ErbB3 gene causes heart valve malformation, whereas trabecula formation is not affected (31). The ErbB family is required also for the maintenance of normal heart function in the adult. Ventricle-specific conditional ErbB2-knockout mice have severe heart failure with dilated ventricles and decreased contractility function. These symptoms resemble human dilated cardiomyopathy (32, 33).

It appears that abnormal regulation of HB-EGF activity in the adult results in cardiovascular pathology such as cardiac hypertrophy (17), smooth muscle cell hyperplasia (18), and pulmonary hypertension (21). To determine the cardiovascular function of HB-EGF in normal mouse development, mice lacking HB-EGF genes were generated by using a targeted gene replacement strategy. In this report we show that HB-EGF-null mice ($HB^{del/del}$) develop severe heart failure associated with dilated ventricular

This paper was submitted directly (Track II) to the PNAS office.

Abbreviations: EGF, epidermal growth factor; HB-EGF, heparin-binding EGF-like growth factor; EGFR, EGF receptor; NRG, neuregulin; LV, left ventricle; RV, right ventricle; LVDd, LV end-diastolic; LVDs, LV end-systolic; E19.5, embryonic day 19.5.

†R.I., S.Y., M.A., and S.T. contributed equally to this work.

††To whom correspondence should be addressed. E-mail: emekada@biken.osaka-u.ac.jp.

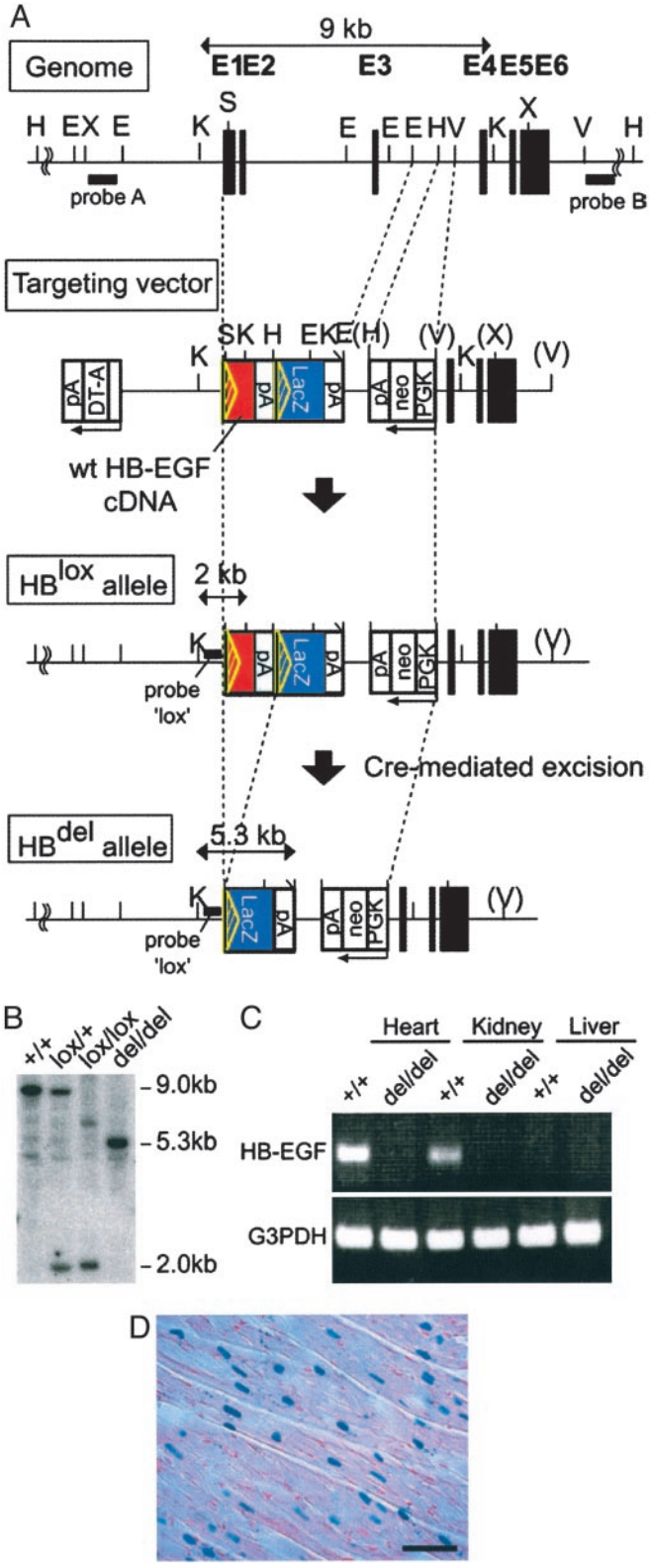

Fig. 1. Generation of HB-EGF-null mice. (*A*) Gene-targeting strategy. Mouse HB-EGF cDNA containing the polyadenylation (pA) sequence flanked by *loxP* sequences was fused with the first exon of the mouse HB-EGF gene. The *lacZ* gene was inserted downstream of the HB-EGF cDNA. The targeting vector also contains the neomycin-resistance gene (*neo*), driven by the phosphoglycerate kinase (PGK) promoter, and the diphtheria toxin A-fragment (DT-A) gene. Cre-mediated recombination results in the deletion of HB-EGF cDNA and in the expression of the *lacZ* gene. Exon sequences are indicated as black boxes. cDNAs encoding HB-EGF and LacZ are indicated as red and blue boxes, respectively. The loxP sites are indicated by yellow-hatched triangles. E, *Eco*RI; H, *Hin*dIII; K, *Kpn*I; S, *Sac*II; V, *Eco*RV; X, *Xho*I. (*B*) Southern blot analysis of the recombination of the HB^{lox} allele. Genomic DNA from tails of WT (+/+), $HB^{lox/+}$ (lox/+), $HB^{lox/lox}$ (lox/lox), and $HB^{del/del}$ (del/del) adult mice was digested with *Kpn*I and hybridized with a *lox* probe. This probe yields a 9.0-kb fragment from the WT allele, a 2.0-kb fragment from the HB^{lox} allele, and a 5.3-kb fragment from the HB^{del} allele. (*C*) RT-PCR analysis of the expression of HB-EGF in WT (+/+) and $HB^{del/del}$ (del/del) mice. Transcripts encoding HB-EGF were observed in the heart and kidney, but not in the liver, of WT mice. No HB-EGF transcripts were found in $HB^{del/del}$ mice. GAPDH (G3PDH) mRNA was measured as a control for RNA preparation. (*D*) HB-EGF LacZ staining of a 12-wk-old $HB^{del/+}$ heart section. (Bar = 50 μm.)

chambers, diminished cardiac function, and grossly enlarged cardiac valves. The cardiac valve and the ventricular chamber defects in HB-EGF-null mice resemble the heart defects displayed by mice lacking EGFR and by mice conditionally lacking ErbB2, respectively. Together, these results suggest that HB-EGF-mediated signaling by means of its ErbB receptors is essential for normal heart development.

Materials and Methods

Generation of HB-EGF-Null Mice. The targeting construct is depicted in Fig. 1*A*. A 7.0-kb *Eco*RI–*Sac*II fragment containing exon 1 of the HB-EGF gene, a 1.3-kb *Eco*RI–*Hin*dIII fragment from intron 3, and a 6.0-kb *Eco*RV fragment downstream of the exon 4 were used as homology arms. Mouse HB-EGF cDNA and a poly(A) signal flanked by *loxP* were fused at exon 1. A 4.0-kb *Hin*dIII–*Xho*I fragment containing the *loxP-lacZ* gene-poly(A) signal was inserted downstream of the HB-EGF cDNA. A *neo* cassette driven by the phosphoglycerate kinase promoter was inserted between the 1.3-kb intron 3 *Eco*RI–*Hin*dIII fragment and the 6.0-kb *Eco*RV fragment downstream of exon 4. *Xho*I-linearized DNA of the targeting vector was electroporated into TT2 embryonic stem (ES) cells. Individual clones were screened for homologous recombination by Southern blot analysis of *Hin*dIII-digested DNA with probes A and B, corresponding to sequences that flank the targeting vector 5′- and 3′-arm, respectively, used in the screening of the HB^{lox} allele. The targeted ES clones were injected into ICR blastocysts, and the chimeric mice were bred with C57BL/6J female mice to obtain $HB^{lox/+}$ mice. Homozygous $HB^{lox/lox}$ mice were obtained by interbreeding of $HB^{lox/+}$ mice. Subsequently, homozygous $HB^{lox/lox}$ mice were bred with CAG-Cre mice (34) to generate $HB^{del/+}$ mice. Finally, $HB^{del/+}$ heterozygous mice were intercrossed to generate HB-EGF-null ($HB^{del/del}$) mice. Deletion of HB-EGF was confirmed by Southern blot analysis of *Kpn*I-digested DNA with a *lox* probe (Fig. 1*A*). RT-PCR was performed by using a reverse transcriptase, ReverTra Dash (Toyobo, Osaka), using forward primer p1 (5′-ATGAAGCTGCTGCCGTCGGT-3′) and reverse primer p2 (5′-TCAGTGGGAGCTAGCCACGC-3′) for the WT proHB-EGF gene transcript, and GAPDH forward primer (5′-ACCACAGTCCATGCCATCAC-3′) and GAPDH reverse primer (5′-TCCACCACCCTGTTGCTGTA-3′) for GAPDH.

Histological Analysis. Mouse tissues were fixed by perfusion of 4% paraformaldehyde, dehydrated, and embedded in paraffin. Four-micrometer sections were stained with hematoxylin/eosin. For LacZ staining, after fixation with 0.2% glutaraldehyde and 1% formalin, tissues were stained with 5-bromo-4-chloro-3-indolyl β-D-galactoside (X-Gal). The stained tissues were fixed again with 3.7% formalin and embedded in paraffin. Four-micrometer sections were stained with nuclear fast red. The myocyte cross-sectional area and the largest diameters of the cardiac valve leaflets in serial sections were measured microscopically.

Echocardiography. Transthoracic echocardiography was performed on unanesthetized mice with a cardiac ultrasound recorder (SONOS 5500, Hewlett–Packard) and a 15-MHz trans-

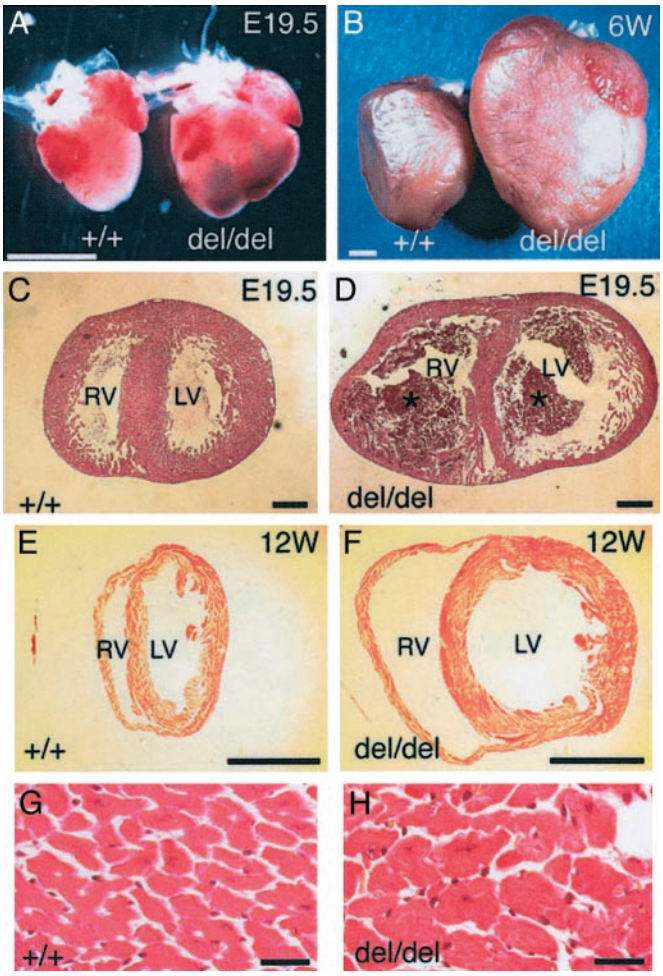

Fig. 2. HB-EGF-null mice have heart defects. (*A*) Representative embryonic day 19.5 (E19.5) WT (+/+) and $HB^{del/del}$ (del/del) hearts. (*B*) Representative 6-wk-old WT (+/+) and $HB^{del/del}$ (del/del) hearts. (*C–H*) Hematoxylin/eosin staining of transverse sections of hearts at the papillary muscle level. (*C* and *D*) WT and $HB^{del/del}$ hearts, respectively, from an E19.5 embryo. (*E* and *F*) WT and $HB^{del/del}$ hearts, respectively, from 12-wk-old mice. In *D* blood clots are indicated by asterisks. (*G* and *H*) High-magnification pictures of *E* and *F*, respectively. (Bars = 2 mm in *A* and *B*, 300 μm in *C* and *D*, 3 mm in *E* and *F*, and 20 μm in *G* and *H*.)

ducer. Images (2D) were acquired in the parasternal short axis, and M-mode (motion mode) images were generated at the level of the papillary muscles to examine motion of cardiac structures as a function of time. The percentage change in left ventricle (LV) diameter during shortening was measured as an assessment of LV function. LV end-diastolic (LVDd) and LV end-systolic (LVDs) internal dimensions were measured and the left ventricular percentage fractional shortening (%FS) was calculated as $\%FS = [(LVDd - LVDs)/LVDd] \times 100$.

Autophosphorylation of ErbB Receptors in HB-EGF-Perfused Mice. Mice were anesthetized with pentobarbital sodium salt (50 mg/kg). Recombinant HB-EGF (R & D Systems), 5 μg/ml in 5 ml of DMEM prewarmed at 37°C, was perfused into the left ventricular chamber of living hearts of WT mice (12-wk C57BL/6J) for 5 min. DMEM alone served as a control. After perfusion, hearts were homogenized in lysis buffer (60 mM octyl β-D-glucoside/0.5 M NaCl/20 mM Hepes-NaOH, pH 7.2/10 mM EDTA/1 mM PMSF/1 mM sodium vanadate/20 μg/ml antipain/10 μg/ml chimostatin/1 μM pepstatin A) on ice by using a Polytron (Kinematica, Lucerne, Switzerland). After centrifugation at 20,000 $\times$ *g* for 30 min, the supernatant was precleared with anti-mouse IgG (Cappel)-conjugated Sepharose 4B. ErbB family members were immunoprecipitated from precleared lysates containing equal amounts of protein, with anti-EGFR, anti-ErbB2, anti-ErbB3, or anti-ErbB4 Ab (Santa Cruz Biotechnology) as primary Ab, and anti-rabbit IgG (Cappel)-conjugated Sepharose 4B as secondary Ab. Immunoprecipitated samples were analyzed by Western blotting using horseradish peroxidase-conjugated anti-phosphotyrosine Ab (Transduction Laboratories), anti-ErbB family Ab, and horseradish peroxidase-conjugated anti-rabbit Ab (Zymed).

Results

Generation of HB-EGF-Null Mice. The strategy for generating HB-EGF-null mice by a conditional targeted gene knockout is shown in Fig. 1. The targeting vector contains WT HB-EGF cDNA flanked by *loxP* sites linked to a *lacZ* reporter gene (Fig. 1*A*). This vector was introduced into mouse ES cells to generate heterozygous mice carrying the HB^{lox} allele. Chimeric mice were bred with C57BL/6J mice to produce heterozygous mice ($HB^{lox/+}$). Homozygous ($HB^{lox/lox}$) mice were identified by PCR analysis (data not shown) and Southern blot analysis (Fig. 1*B*). No overt abnormality was observed in either $HB^{lox/+}$ or $HB^{lox/lox}$ mice.

To generate mice lacking the HB-EGF gene, $HB^{lox/lox}$ mice were crossed with CAG-Cre transgenic mice (34). The Cre-mediated recombination in F_1 mice occurs before the two-cell stage of embryonic development. Because the recombination could be due to maternal CAG-Cre recombinase in an oocyte, $HB^{del/+}$ mice that did not possess the CAG-Cre transgene were obtained by breeding female CAG-Cre transgenic mice with male $HB^{lox/lox}$ mice. There is no evidence that strong expression of Cre recombinase induces abnormalities in mice. In addition, no overt abnormality was observed in heterozygous HB-EGF-null ($HB^{del/+}$) mice. The $HB^{del/+}$ mice lacking the CAG-Cre transgene were used to generate homozygous HB-EGF-null ($HB^{del/del}$) mice. $HB^{del/del}$ mice were

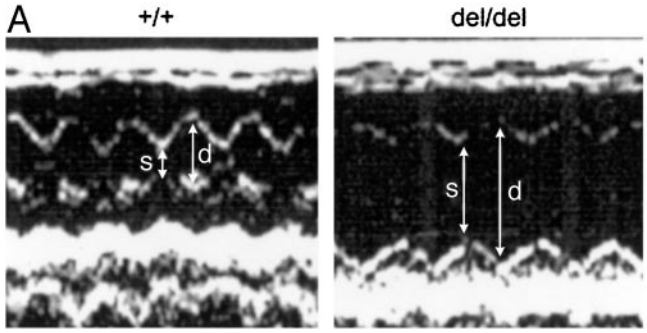

B

	+/+ (*n* = 7)	del/del (*n* = 8)	*P*-value
BW, g	21.7 +/- 1.3	20.5 +/- 0.8	n.s.
HR, /min	662.7 +/- 24.3	619.3 +/- 22.1	n.s.
sBP, mmHg	110.4 +/- 2.6	103.9 +/- 5.0	n.s.
dBP, mmHg	73.3 +/- 4.9	64.7 +/- 3.7	n.s.
LVDd, mm	2.87 +/- 0.13	4.53 +/- 0.32	<0.001
LVDs, mm	1.48 +/- 0.14	3.26 +/- 0.33	<0.001
FS, %	49.1 +/- 2.8	29.2 +/- 3.3	<0.001

Fig. 3. Echocardiography. (*A*) representative records of 2D echocardiograms of WT (+/+) and $HB^{del/del}$ (del/del) mice. Arrows indicate the end-diastolic (d) and end-systolic (s) dimensions, respectively. (*B*) Physiological parameters of 8- to 12-wk-old mice. BW, body weight; HR, heart rate; sBP and dBP, systolic and diastolic blood pressure, respectively; FS, fractional shortening calculated as $[(LVDd - LVDs)/LVDd] \times 100$; n.s., not significant. All values are ±SEM.

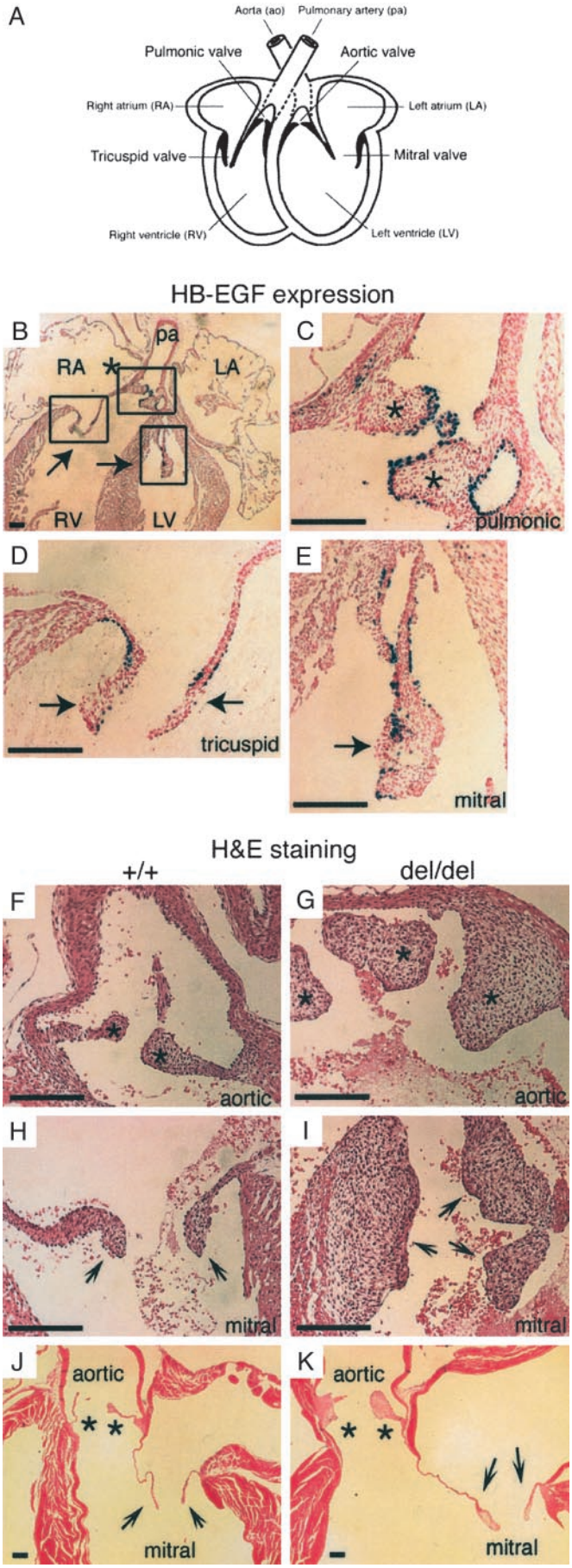

identified by PCR analysis (data not shown) and Southern blot analysis (Fig. 1*B*). RT-PCR analysis of total RNA from adult heart and kidney confirmed the absence of proHB-EGF message in $HB^{del/del}$ mice (Fig. 1*C*).

A targeting vector containing the *lacZ* gene as a reporter for the expression of HB-EGF was prepared. The *lacZ* gene is silent in $HB^{lox/lox}$ mice but is driven by the native HB-EGF promoter when HB-EGF cDNA is deleted by Cre recombinase (Fig. 1*A*). Thus, it is possible in homozygous and heterozygous mice to histochemically identify cells expressing HB-EGF by staining for LacZ. The LacZ construct contains the nuclear targeting signal (NTR-LacZ), and cells expressing HB-EGF can be readily identified by staining the nuclei with 5-bromo-4-chloro-3-indolyl β-D-galactoside (X-Gal). The expression of HB-EGF in cardiomyocytes of 12-wk-old $HB^{del/+}$ mice could be detected by LacZ staining (Fig. 1*D*). More than 50% of the cardiomyocytes were LacZ-positive, indicating that cardiomyocytes express HB-EGF.

Targeted Disruption of HB-EGF Causes Cardiac Dysfunction. Breeding of heterozygous male and female mice yielded HB-EGF-null mice ($HB^{del/del}$). More than 60% of the homozygous mice died in the first postnatal week. Although the $HB^{del/del}$ survivors showed no obvious outer abnormality, they had shorter lifespans compared with control littermates. More than half of the $HB^{del/del}$ survivors died postnatally at 25 days. Autopsies of 6-wk-old $HB^{del/del}$ mice showed massive enlargement of the heart (Fig. 2*B*). Heart enlargement could be detected even by E19.5 (Fig. 2*A*).

Histological analysis of E19.5 $HB^{del/del}$ embryos demonstrated that both left and right ventricular chambers were dilated (Fig. 2*D*) compared with control hearts (Fig. 2*C*). Adult $HB^{del/del}$ mice (12 wk old) also demonstrated progressive ventricular dilation of both chambers (Fig. 2 *F* vs. *E*). In either case, no significant differences were observed in the body weights of WT compared with $HB^{del/del}$ mice (data not shown). In addition, the size of cardiomyocytes was enlarged by approximately 2-fold in 12-wk-old $HB^{del/del}$ mice (Fig. 2*H*) compared with control mice (Fig. 2*G*). The average cross-sectional areas of $HB^{del/del}$ cardiomyocytes were $393 \pm 39.2\ \mu m^2$ in 12-wk hearts ($n = 4$), and $194 \pm 33.9\ \mu m^2$ for the hearts of WT littermates ($n = 5$; $P < 0.0001$). However, at E19.5, no difference was observed in the size of $HB^{del/del}$ and control cardiomyocytes (data not shown), indicating that hypertrophy of the cardiomyocytes did not occur yet at this stage. At no point in development of $HB^{del/del}$ hearts was infiltration of mononuclear cells and macrophages observed, suggesting that neither inflammatory nor autoimmune responses were involved in promoting the abnormal cardiac phenotype.

Cardiovascular function was evaluated by transthoracic echocardiography (Fig. 3*A*). Typically, a high degree of dilation of the LV of $HB^{del/del}$ mice was observed in echocardiograms. Physiological parameters are shown in Fig. 3*B*. At 8–12 wk, the enlarged left ventricular diameters had an average value of 4.53 mm in $HB^{del/del}$ mice and 2.87 mm in control mice (Fig. 3*B*). The ventricular fractional shortening (FS), a measure of systolic function, was

Fig. 4. Cardiac valve defects in $HB^{del/del}$ mice. (*A*) Schematic illustration of the heart depicting positions of the valves. (*B–E*) LacZ staining of longitudinal sections through the hearts of E19.5 $HB^{del/+}$ (corresponds to WT) embryos. (*B*) HB-EGF is expressed at the margins of the pulmonic valve (asterisks) and in tricuspid and mitral valves (arrows). pa, pulmonary artery. (*C–E*) Higher magnification of areas indicated by the boxes in *B*. Pulmonic valve (*C*, asterisks), tricuspid valve (*D*, arrows), and mitral valve (*E*, arrow) are shown. (*F–K*) Histological analysis of cardiac valves. Shown are hematoxylin/eosin-stained longitudinal sections of hearts of E19.5 embryos (*F–I*) and of 12-wk-old mice (*J* and *K*). Mice are WT (*F*, *H*, and *J*) and $HB^{del/del}$ (*G*, *I*, and *K*). E19.5 aortic valves (*F* and *G*, asterisks), E19.5 mitral valves (*H* and *I*, arrows), and 12-wk-old aortic (*J* and *K*, asterisks) and mitral (*J* and *K*, arrows) valves are shown. Pulmonic and tricuspid valves are also enlarged (not shown). (Bars = 150 μm.)

Table 1. Measurement of cardiac valve size

Valve	Diameter, μm			*P* value*		
	+/+ (n = 5)	del/+ (n = 4)	del/del (n = 5)	*P*1	*P*2	*P*3
Pulmonic	107 ± 5.8	110 ± 33.7	196 ± 23.0	n.s.	<0.003	<0.003
Aortic	84 ± 19.5	128 ± 28.7	194 ± 32.1	<0.03	<0.003	<0.02
Tricuspid	58 ± 9.6	70 ± 14.1	224 ± 32.9	n.s.	<0.003	<0.003
Mitral	87 ± 15.3	50 ± 8.2	208 ± 69.1	<0.01	<0.03	<0.003

The largest diameters of each valve in serial sections of E19.5 embryos of wild-type (+/+), $HB^{del/+}$ (del/+), and $HB^{del/del}$ (del/del) hearts were measured. The valve size values are calculated as mean ± SEM.
*The *P* values are *P*1, +/+ versus del/+; *P*2, +/+ versus del/del; and *P*3, del/+ versus del/del; n.s., not significant.

reduced from 49% (WT) to 29% ($HB^{del/del}$). Together, the histopathological and echocardiographic analysis indicated that $HB^{del/del}$ mice displayed increased chamber size, myofiber hypertrophy, and decreased fractional shortening, signs of severe cardiac dysfunction.

Heart Valve Malformation. Heart valves malformations have been observed in EGFR-null (27) and EGFR-mutant (*waved-2*) mice (27). EGFR is a receptor for HB-EGF (3), so the valve defects could be due to loss of HB-EGF activity transduced by EGFR. Accordingly, possible cardiac valve abnormalities in $HB^{del/del}$ mice were investigated. For orientation, a schematic showing the positions of the valves is shown in Fig. 4*A*. LacZ staining of E19.5 $HB^{del/+}$ embryos showed that HB-EGF is expressed strongly at the margins of all of the cardiac valves (Fig. 4 *B–E*). Histological analysis of E19.5 embryonic $HB^{del/del}$ hearts showed enlarged semilunar (aortic and pulmonic) valves (Fig. 4*G*) and atrioventricular (mitral and tricuspid) valves (Fig. 4*I*) with abnormal thickened morphology compared with the control hearts (Fig. 4 *F* and *H*, respectively). The average sizes of the cardiac valves of E19.5 hearts were determined by measuring microscopically the largest diameter of each valve in serial sections (Table 1). Masson-trichrome staining indicated that no particular fibrosis occurred in the enlarged valves (data not shown), suggesting that valve thickening resulted from the increased number of mesenchymal cells. Enlargement of the aortic valves and mitral valves was also detected in the hearts of 12-wk-old adult $HB^{del/del}$ mice (Fig. 4*K*) compared with the control hearts (Fig. 4*J*), although the rate of thickening of the mitral valve was relatively lower than that of the aortic valve.

HB-EGF Signals EGFR, ErbB2, and ErbB4 in the Heart. $HB^{del/del}$ mice share similar cardiac phenotypes as EGFR-knockout and ErbB2 conditional knockout mice, suggesting that HB-EGF functions upstream of EGFR and ErbB2 in the heart. Recombinant soluble HB-EGF was administered into the LV chambers of WT mice. HB-EGF induced strong autophosphorylation of ErbB2 and ErbB4, and induced to a lesser yet substantial degree autophosphorylation of EGFR (Fig. 5*A*). These results demonstrate that HB-EGF signals EGFR, ErbB2, and ErbB4 in the living heart. HB-EGF might activate ErbB4 directly (23), whereas ErbB2 might be an indirect receptor by heterodimerization (2). Constitutive tyrosine phosphorylation of ErbB2 and ErbB4 in WT hearts occurred without HB-EGF stimulation (Fig. 5*A*). Tyrosine phosphorylation levels of both ErbB2 and ErbB4 were significantly reduced in the heart of $HB^{del/del}$ mice compared with those of WT mice even though ErbB2 and ErbB4 protein levels were relatively up-regulated in $HB^{del/del}$ mice (Fig. 5*B*). These results provide further evidence that HB-EGF signals by means of activation of ErbB2 and ErbB4 in the heart.

Discussion

Using HB-EGF-null mice, we have shown that HB-EGF is essential for normal cardiac function. The $HB^{del/del}$ mice display enlarged hearts, hypertrophic cardiomyocytes, and abnormal cardiac valves. In addition, echocardiography shows dilation of cardiac chambers and decreased systolic function. These heart defects might contribute to the early postnatal lethality of HB-EGF-null mice. EGF, transforming growth factor-α, and amphiregulin are the other EGFR ligands that have been targeted (35, 36). However, these knockout mice have never been reported to exhibit an abnormal heart phenotype even when all three were targeted. Thus, HB-EGF plays a role in heart development that is not shared by the other EGFR ligands.

HB-EGF is expressed in late-stage WT embryos at the margin of semilunar valves and at the margin of atrioventricular valves. In late-stage embryos lacking HB-EGF, both semilunar and atrioventricular valves are enlarged with a thickened globular morphology. On the other hand, EGFR-null mice and *waved-2*-defective EGFR mice have enlarged semilunar valves but not enlarged atrioventricular valves (27). Because HB-EGF can activate EGFR directly, this

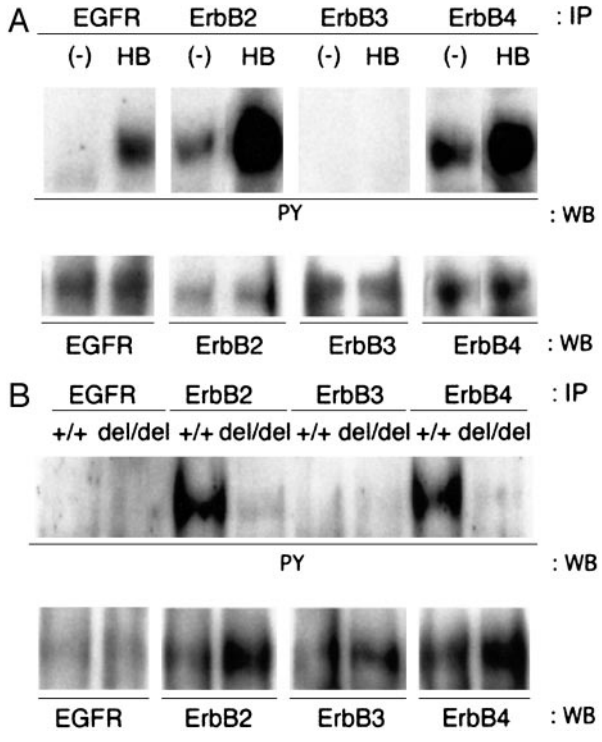

Fig. 5. Tyrosine phosphorylation of the ErbB receptor family. (*A*) DMEM (−) or 5 μg/ml recombinant soluble HB-EGF (HB) was perfused directly into the WT heart. Each ErbB receptor was immunoprecipitated from lysates with its corresponding Ab. The immunoprecipitates (IP) were analyzed by Western blotting (WB) using anti-phosphotyrosine Ab (PY) or each of the four corresponding anti-ErbB Abs. (*B*) Comparison of the constitutive phosphorylation and protein levels of ErbB receptors in WT (+/+) and $HB^{del/del}$ (del/del) hearts. Hearts perfused with DMEM were homogenized and analyzed by immunoprecipitation and Western blotting as in *A*.

growth factor may be essential for the normal development of semilunar valves. In terms of mechanism, HB-EGF might be required for semilunar valve development by regulating the number of endothelial cells transformed into mesenchymal cells, the extent of mesenchymal cell proliferation, or the differentiation of the mesenchyme into mature semilunar valve structures, a process involving apoptosis (27). Because HB-EGF, but not EGFR, is needed for the development of atrioventricular valves, it is possible that other ErbB receptors activated by HB-EGF may be involved in formation of the atrioventricular valves, e.g., by direct interaction of HB-EGF with ErbB4, by interactions of HB-EGF with heterodimers of EGFR with ErbB2, ErbB3, and/or ErbB4, or by HB-EGF interactions with heterodimers of ErbB4 with ErbB2 and/or ErbB3. Interestingly, disruption of ErbB3 causes heart valve malformation (31).

In addition to the abnormal valve formation, $HB^{del/del}$ mice displayed hypertrophy of cardiomyocytes, enlarged ventricular chambers, and reduced fractional shortening. It is possible that these cardiac abnormalities could be induced secondarily by abnormal valve formation. Inefficient pumping caused by a defect in valvulogenesis might induce compensatory responses in the myocytes that result in cardiac remodeling, namely cardiac chamber dilation and myocyte hypertrophy, in an attempt to augment systolic function (37). Secondary hypertrophy and cardiac dysfunction caused by abnormal valves can be observed in the clinic. However, $HB^{del/del}$ mice exhibited ventricular chamber dilation even in E19.5 embryonic hearts, which are not yet subjected to any significant stress and are not capable of fully supporting the circulation, suggesting that the phenotype may not be due to secondary effects on valves.

Ventricular chamber-specific ErbB2 conditional knockout mice exhibit adult cardiomyopathy (32, 33) with symptoms resembling the cardiac phenotype of $HB^{del/del}$ mice, which include ventricular chamber dilation, cardiomyocyte hypertrophy, and reduced fractional shortening. The phenotype of ErbB2 conditional knockout mice is typically attributed to a loss of NRG activity because NRG is a ligand for heterodimers containing ErbB2. However, loss of HB-EGF also could be responsible for this phenotype because it is possible that HB-EGF activates adult cardiomyocyte ErbB2 by means of EGFR/ErbB2 heterodimers or ErbB2/ErbB4 heterodimers. These putative interactions of HB-EGF are a distinct possibility because we have demonstrated that soluble HB-EGF perfused into WT hearts induces tyrosine phosphorylation of EGFR, ErbB2, and ErbB4. Furthermore, the constitutive tyrosine phosphorylation levels of ErbB2 and ErbB4 are reduced significantly in $HB^{del/del}$ mice. The source of HB-EGF that maintains constitutive phosphorylation levels may be the cardiomyocytes that we have shown to express abundant HB-EGF. This evidence suggests that lack of HB-EGF in HB-EGF-null mice might lead to loss of EGFR, ErbB2, and ErbB4 activity.

In conclusion, HB-EGF acting through ErbB tyrosine kinase receptors is a critical growth factor for the maintenance of normal heart function. Further studies are needed to determine the role of HB-EGF and downstream ErbB receptors in cardiomyocyte function and development of cardiac valves.

We thank Dr. G. Yamada (Kumamoto University, Kumamoto, Japan) for producing gene-targeted mice and Dr. J. Miyazaki (Osaka University) for providing the CAG-Cre transgenic mice. We thank Dr. S. Beppu (Osaka University) and Dr. M. Rupnick (Children's Hospital) for the echocardiographic analyses and description. We also thank I. Ishimatsu for expert technical assistance with histological analysis. This work was supported by the Research for the Future Program of the Japan Society for the Promotion of Science and by Grants-in-Aid from the Ministry of Education, Culture, Sports, Science and Technology (to E.M.). M.A. is a recipient of the Japan Society for the Promotion of Science Research Fellowship.

1. Olayioye, M. A., Neve, R. M., Lane, H. A. & Hynes, N. E. (2000) *EMBO J.* **19,** 3159–3167.
2. Tzahar, E. & Yarden, Y. (1998) *Biochim. Biophys. Acta* **1377,** M25–M37.
3. Higashiyama, S., Abraham, J. A., Miller, J., Fiddes, J. C. & Klagsbrun, M. A. (1991) *Science* **251,** 936–939.
4. Higashiyama, S., Lau, K., Besner, G. E., Abraham, J. A. & Klagsbrun, M. (1992) *J. Biol. Chem.* **267,** 6205–6212.
5. Goishi, K., Higashiyama, S., Klagsbrun, M., Nakano, N., Umata, T., Ishikawa, M., Mekada, E. & Taniguchi, N. (1995) *Mol. Biol. Cell* **6,** 967–980.
6. Higashiyama, S., Iwamoto, R., Goishi, K., Raab, G., Taniguchi, N., Klagsbrun, M. & Mekada, E. (1995) *J. Cell Biol.* **128,** 929–938.
7. Iwamoto, R., Handa, K. & Mekada, E. (1999) *J. Biol. Chem.* **274,** 25906–25912.
8. Iwamoto, R. & Mekada, E. (2000) *Cytokine Growth Factor Rev.* **11,** 335–344.
9. Mitamura, T., Iwamoto, R., Umata, T., Yomo, T., Urabe, I., Tsuneoka, M. & Mekada, E. (1992) *J. Cell Biol.* **118,** 1389–1399.
10. Nakamura, K., Iwamoto, R. & Mekada, E. (1995) *J. Cell Biol.* **129,** 1691–1705.
11. Naglich, J. G., Metherall, J. E., Russell, D. W. & Eidels, L. (1992) *Cell* **69,** 1051–1061.
12. Iwamoto, R., Higashiyama, S., Mitamura, T., Taniguchi, N., Klagsbrun, M. & Mekada, E. (1994) *EMBO J.* **13,** 2322–2330.
13. Higashiyama, S., Abraham, J. A. & Klagsbrun, M. (1993) *J. Cell Biol.* **122,** 933–940.
14. Raab, G. & Klagsbrun, M. (1997) *Biochim. Biophys. Acta* **1333,** F179–F199.
15. Marikovsky, M., Breuing, K., Liu, P. Y., Eriksson, E., Higashiyama, S., Farber, P., Abraham, J. & Klagsbrun, M. (1993) *Proc. Natl. Acad. Sci. USA* **90,** 3889–3893.
16. Tokumaru, S., Higashiyama, S., Endo, T., Nakagawa, T., Miyagawa, J., Yamamori, K., Hanakawa, Y., Ohmoto, H., Yoshino, K., Shirakata, Y., *et al.* (2000) *J. Cell Biol.* **151,** 209–220.
17. Asakura, M., Kitakaze, M., Takashima, S., Liao, Y., Ishikura, F., Yoshinaka, T., Ohmoto, H., Node, K., Yoshino, K., Ishiguro, H., *et al.* (2002) *Nat. Med.* **8,** 35–40.
18. Miyagawa, J., Higashiyama, S., Kawata, S., Inui, Y., Tamura, S., Yamamoto, K., Nishida, M., Nakamura, T., Yamashita, S., Matsuzawa, Y., *et al.* (1995) *J. Clin. Invest.* **95,** 404–411.
19. Takemura, T., Hino, S., Kuwajima, H., Yanagida, H., Okada, M., Nagata, M., Sasaki, S., Barasch, J., Harris, R. C. & Yoshioka, K. (2001) *J. Am. Soc. Nephrol.* **12,** 964–972.
20. Das, S. K., Wang, X.-N., Paria, B. C., Damm, D., Abraham, J. A., Klagsbrun, M., Andrews, G. K. & Dey, S. K. (1994) *Development (Cambridge, U.K.)* **120,** 1071–1083.
21. Lemjabbar, H. & Basbaum, C. (2002) *Nat. Med.* **8,** 41–46.
22. Fu, S., Bottoli, I., Goller, M. & Vogt, P. K. (1999) *Proc. Natl. Acad. Sci. USA* **96,** 5716–5721.
23. Elenius, K., Paul, S., Allison, G., Sun, J. & Klagsbrun, M. (1997) *EMBO J.* **16,** 1268–1278.
24. Nishi, E., Prat, A., Hospital, V., Elenius, K. & Klagsbrun, M. (2001) *EMBO J.* **20,** 3342–3350.
25. Prenzel, N., Zwick, E., Daub, H., Leserer, M., Abraham, R., Wallasch, C. & Ullrich, A. (1999) *Nature* **402,** 884–888.
26. Eguchi, S., Dempsey, P. J., Frank, G. D., Motley, E. D. & Inagami, T. (2001) *J. Biol. Chem.* **276,** 7957–7962.
27. Chen, B., Bronson, R. T., Klaman, L. D., Hampton, T. G., Wang, J. F., Green, P. J., Magnuson, T., Douglas, P. S., Morgan, J. P. & Neel, B. G. (2000) *Nat. Genet.* **24,** 296–299.
28. Lee, K. F., Simon, H., Chen, H., Bates, B., Hung, M. C. & Hauser, C. (1995) *Nature* **378,** 394–398.
29. Meyer, D. & Birchmeier, C. (1995) *Nature* **378,** 386–390.
30. Gassmann, M., Casagranda, F., Orioli, D., Simon, H., Lai, C., Klein, R. & Lemke, G. (1995) *Nature* **378,** 390–394.
31. Erickson, S. L., O'Shea, K. S., Ghaboosi, N., Loverro, L., Frantz, G., Bauer, M., Lu, L. H. & Moore, M. W. (1997) *Development (Cambridge, U.K.)* **124,** 4999–5011.
32. Ozcelik, C., Erdmann, B., Pilz, B., Wettschureck, N., Britsch, S., Hubner, N., Chien, K. R., Birchmeier, C. & Garratt, A. N. (2002) *Proc. Natl. Acad. Sci. USA* **99,** 8880–8885.
33. Crone, S. A., Zhao, Y.-Y., Fan, L., Gu, Y., Minamisawa, S., Liu, Y., Peterson, K. L., Ju, C., Kahn, R., Condorelli, G., *et al.* (2002) *Nat. Med.* **8,** 459–465.
34. Sakai, K. & Miyazaki, J. (1997) *Biochem. Biophys. Res. Commun.* **237,** 318–324.
35. Luetteke, N. C., Qiu, T. H., Fenton, S. E., Troyer, K. L., Riedel, R. F., Chang, A. & Lee, D. C. (1999) *Development (Cambridge, U.K.)* **126,** 2739–2750.
36. Mann, G. B., Fowler, K. J., Gabriel, A., Nice, E. C., Williams, R. L. & Dunn, A. R. (1993) *Cell* **73,** 249–261.
37. Chien, K. R. (1999) *Cell* **98,** 555–558.